Analysis of Two Dimensional and Three Dimensional Supersonic Turbulence Flow around Tandem Cavities

Chel Hun Woo
Department of Aerospace Engineering, Chosun University, GwangJu 501-759, Korea
Jae Soo Kim*
Corresponding author, Department of Aerospace Engineering, Chosun University, GwangJu 501-759, Korea
Kyung Hwan Lee
Department of Aerospace Engineering, Sunchon National University, Sunchon, 540-742, Korea

The supersonic flows around tandem cavities were investigated by two-dimensional and three-dimensional numerical simulations using the Reynolds-Averaged Navier-Stokes (RANS) equation with the $k-\omega$ turbulence model. The flow around a cavity is characterized as unsteady flow because of the formation and dissipation of vortices due to the interaction between the freestream shear layer and cavity internal flow, the generation of shock and expansion waves, and the acoustic effect transmitted from wake flow to upstream. The upwind TVD scheme based on the flux vector split with van Leer's limiter was used as the numerical method. Numerical calculations were performed by the parallel processing with time discretizations carried out by the 4th-order Runge-Kutta method. The aspect ratios of cavities are 3 for the first cavity and 1 for the second cavity. The ratio of cavity interval to depth is 1. The ratio of cavity width to depth is 1 in the case of three dimensional flow. The Mach number and the Reynolds number were 1.5 and 4.5×10^5, respectively. The characteristics of the dominant frequency between two-dimensional and three-dimensional flows were compared, and the characteristics of the second cavity flow due to the first cavity flow was analyzed. Both two dimensional and three dimensional flow oscillations were in the 'shear layer mode', which is based on the feedback mechanism of Rossiter's formula. However, three dimensional flow was much less turbulent than two dimensional flow, depending on whether it could inflow and outflow laterally. The dominant frequencies of the two dimensional flow and three dimensional flows coincided with Rossiter's 2nd mode frequency. The another dominant frequency of the three dimensional flow corresponded to Rossiter's 1st mode frequency.

Key Words: Tandem Cavity flow, Unsteady 3-Dimensional Supersonic Turbulence Flow, $k-\omega$ Turbulence Model, Dominant Frequency Analyses, 4th-Order Runge-Kutta Method

* Corresponding Author,
E-mail : jsckim@mail.chosun.ac.kr
TEL : +82-62-230-7080; **FAX** : +82-62-223-8894
Corresponding author, Department of Aerospace Engineering, Chosun University, GwangJu 501-759, Korea.
(Manuscript **Received** November 30, 2005; **Revised** April 27, 2006)

1. Introduction

The high-speed flight vehicles have cavities such as wheel wells and bomb bays. The supersonic cavity flow is complicated due to vortices, flow separation and reattachment, and shock and

expansion waves. The main characteristic of cavity flow is the vortices inside cavity generated from the collision of the unstable shear layer formed at the cavity leading edge to the cavity trailing edge or to the cavity floor as the flow passes the cavity. Such a collision transmits sound waves upstream and affects the shear layer at the leading edge to create a flow circulation that induces oscillation. This type of circulation process was suggested by Rossiter (1964), whose formula for the prediction of resonance frequency is still widely used. This type of cavity flow shows unsteady three dimensional flow characteristics even for the cavities with a small aspect ratio (ratio of length to depth, L/D). The general cavity flow phenomena include the formation and dissipation of vortices, which induce oscillation and noise. The oscillation and noise greatly affect flow control, chemical reaction, and heat transfer processes. The supersonic cavity flow with high Reynolds number is characterized by the pressure oscillation due to turbulent shear layer, cavity geometry, and resonance phenomenon based on external flow conditions. The resonance phenomena can damage the structures around the cavity and negatively affect aerodynamic performance and stability (Baysal and Stallings, 1998 ; Maull and East, 1963).

The supersonic cavity flow can be classified into two types, as shown in Fig. 1 : open type ($L/D<10$) and closed type ($L/D>13$). In the open cavity flow, the shear layer reattaches at the cavity trailing edge, and thus, the interaction between the freestream shear layer and external flow produces severe pressure variations and flow fluctuations. The oscillations occur spanwisely, longitudinally, and transversely, which induce serious noise and structural problems. In the closed cavity flow, the shear layer formed between the high speed external flow and low speed internal flow

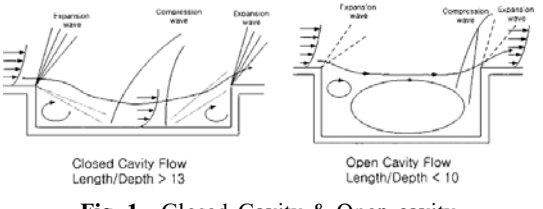

Fig. 1 Closed Cavity & Open cavity

expands as it passes the cavity and collides with the cavity floor. The oscillation due to pressure variations in closed cavity flow is not as severe as that in the open cavity flow. Therefore, the expansion waves are generated at the leading edge and the shear layer that collided with the cavity floor forms continuous shock waves. It moves to the top and escapes from the trailing edge. As a result, two separation regimes are formed at the forward and backward of cavity (Xin and Edwards, 1992 ; 1995).

Rossiter (1964), Xin Zhang and Edwards (1992, 1995), Krishnamurty (1995) and Heller (1971) confirmed that the pressure oscillations of cavity flow are produced by the periodic and random components of flow. Generally, flow characteristics are dependent on the incoming boundary layer, cavity geometry, flow velocity, and many other parameters. The mechanism of noise generation is dependent on cavity depth. Gharib and Roshko (1987) demonstrated that the shear layer mode changes to wake mode in two dimensional cavity flow, as the ratio of length to depth (L/D) increases. Also, in three dimensional cavity flow, the shear layer mode is predominant in comparison with the wake mode (Chingwei and Philip, 2001). In the shear layer mode, the unstable shear layer collides with the cavity trailing edge wall, whereas the flow separated at the cavity leading edge periodically collides with the cavity floor and moves out the cavity in the wake mode, which shows that the wake mode flow is very violent.

Most researches on cavities have been limited to the two-dimensional single cavity (Xin Zhang and Edwards, 1992 ; 1995). A few of researches are focused on three-dimensional single cavity or two-dimensional double cavity flows (Chingwei and Philip, 2001 ; Hwang, 1994). However, since the real flight vehicles have two tandem cavities, there have been many researches on such structures recently. Xin Zhang and Edwardsd (1992 ; 1995) investigated the supersonic flow around two dimensional tandem cavities with different aspect ratios. Hwang (1994) carried out experiments and numerical analysis on two dimensional tandem cavities with different aspect ratios by the Baldwin-Lomax turbulence model.

In the present study, the numerical analysis on three dimensional tandem cavities flow was performed by the unsteady compressible Reynolds-Averaged Navier-Stokes (RANS) equations with the $k-\omega$ turbulence model. The Strouhal numbers of the first and second cavities were compared and verified by Rossiter's equation (1964) and experimental values of Xin Zhang and Edwards (1992 ; 1995). The cavity model used for numerical calculation had a depth (D) of 15 mm, first cavity L/D of 3, second cavity L/D of 1, and cavity interval of S/D of 1 (Xin Zhang and Edwards, 1992 ; 1995). The supersonic flow had a Reynolds number of 4.5×10^5 based on cavity depth, and Mach number of 1.5. The same basic flow conditions were applied for two dimensional and three dimensional analyses. The width to depth ratio (W/D) was 1.0 for three dimensional analysis. The parallel numerical analysis was carried out, which used the 4th order Runge-Kutta method for time discretization and the second order upwind TVD scheme using the flux vector splits with van Leer's limiter for spatial discretization.

Based on the PSD (Power Spectral Density) analysis of the pressure variation at the first cavity floor, the dominant frequency was reasonable in comparison with the results of Rossiter (1964) and Xin Zhang and Edwards (1995). The dominant frequency of the second cavity followed that of the first cavity. This result was in agreement with the results of Xin Zhang and Edwards (1992). In two dimensional flow, the dominant frequency is almost same to the 2nd mode dominant frequency of Rossiter's equation (1964). The 1st mode dominant frequency as well as the 2nd mode frequency appears in the three dimensional flow due to the lateral inflow and outflow, which makes that the three dimensional flow inside the cavity was less violent than the two dimensional flow.

2. Governing Equations and Numerical Method

Three dimensional Navier-Stokes equation non-dimensionalized by the characteristic values is as follows :

$$\frac{\partial \bar{Q}}{\partial t}+\frac{\partial \bar{E}}{\partial \xi}+\frac{\partial \bar{F}}{\partial \eta}+\frac{\partial \bar{G}}{\partial \zeta} =\frac{\partial \overline{E_v}}{\partial \zeta}+\frac{\partial \overline{F_v}}{\partial \eta}+\frac{\partial \overline{G_v}}{\partial \zeta}+\bar{S} \quad (1)$$

The cavity depth (D), freestream velocity (U_∞), and freestream density (ρ_∞) are the characteristic values. The non-dimensional time and generalized coordinates are indicated as t, ξ, η, ζ, respectively. $\bar{Q}$ is the non-dimensional flux vector Q/J $(=(\rho, \rho u, \rho v, \rho w, \rho e)^T/J)$, converted to generalized coordinates. $\bar{E}$, $\bar{F}$, $\bar{G}$ and $\overline{E_v}$, $\overline{F_v}$, $\overline{G_v}$ are the generalized coordinate flux vectors expressed as functions of the transform matrix. Inviscid flux vectors Q, E, F, G, viscous flux vectors E_v, F_v, G_v and other symbols are the same as those in the reference (Hoffmann and Chiang, 1993). $\bar{S}$ is the source term used in turbulence model. The $k-w$ model was adapted as the turbulence model. The equations can be expressed in generalized coordinates in conservation form like the Navier-Stokes equation. The turbulence formula vectors corresponding to each flux vector of the Navier-Stokes equation are as those in the reference (David and Wilcox, 2000 ; Pao and Abdol-Hamid, 1996). The compressibility correction function proposed by Sarkar (1991) are applied.

The 4th order Runge-Kutta method was used for the time discretization and the coeffieients for Runge-Kutta was 1/4, 1/6, 3/8, and 1 (Hoffmann and Chiang, 1993). The van Leer's FVS was used for the spacial discretization. The parallel process by PC-cluster was used for calculations (Woo and Kim, 2005).

3. Result and Discussion

3.1 Problem definition and grid system

The numerical analysis of two dimensional and three dimensional unsteady supersonic flow around tandem cavities was performed with the cavity geometry and the flow condition obtained from the experimental model of Xin Zhang and Edwards (1992 ; 1995). The model cavities had a depth (D) of 15 mm, first cavity L/D of 3, second cavity L/D of 1, and cavity interval of S/D of 1. The supersonic flow had a Reynolds number of 4.5×10^5 based on cavity depth and Mach number

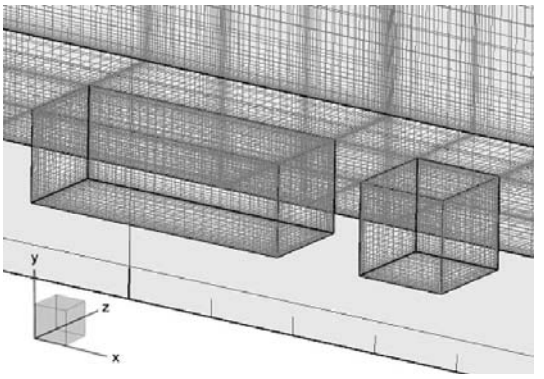

Fig. 2 Computational grids for the three dimensional calculation

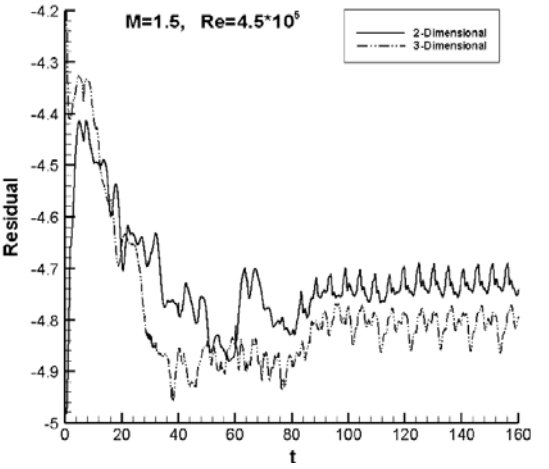

Fig. 3 Residual histories

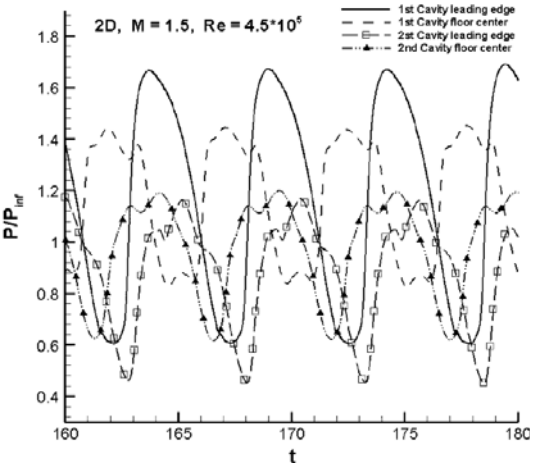

Fig. 4 Pressure histories at the two dimensional cavity flow

of 1.5. Basic flow conditions were the same for both two dimensional and three dimensional analyses, and the width to depth (W/D) was 1.0 for three dimensional analysis.

Figure 2 shows a part of the three dimensional grid system around the cavity. The grid was concentrated near the wall. For two dimensional analysis, the grid number for upper zone was 350×100, for the first cavity 100×70, and for the second cavity 50×70. For three dimensional analysis, the grid numbers were $140\times40\times40$, $50\times30\times20$, and $30\times30\times20$, respectively. The far field length is about 7D. The $y^+(=y\sqrt{\rho_w\tau_w}/\mu_w)$ of first grid is about 0.001～1.5. Abdol-Hamid (1975) etc. present very reasonable results in the case of separated flow when the y^+ of first grid is less than 10. Although several numerical tests have been done with more fine grids, there are no significant differences in the results of dominant frequency analysis. Even though it is not enough to show the detail turbulence sublayer, it seems to show very reasonable results in the flow field without a wall function.

3.2 Two dimensional and three dimensional flow analysis and comparison

Figure 3 show the residual variation according to the non-dimensional time for two dimensional and three dimensional flows. The random oscillation vanishes and periodic oscillation appears after the non-dimensional time about $t=100$. The residual period time is 5.2 for two dimensional flow and about 10.4 for three dimensional flow, which reflect the flow oscillation period. The period of three dimensional flow is twice as long as that of two dimensional flow, whose reason can be predicted from the difference in the pressure histories in Figs. 4～6.

Figures 4～6 show the pressure histories at several locations on two dimensional and three dimensional cavities, respectively. The sloid lines and long-dashed-square lines show the pressure histories at the cavity leading edges of $(x/D,\ y/D,\ z/D)=(0.0,\ 1.0,\ 0.5)$ and $(4.0,\ 1.0,\ 0.5)$. The dashed lines and dashed-dot -triangle lines show the pressure histories at the cavity floor

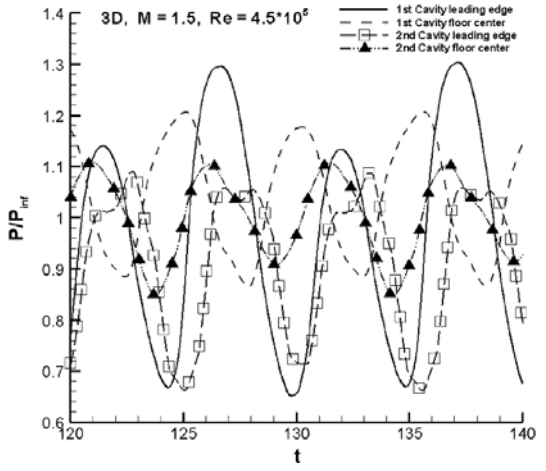

Fig. 5 Pressure histories at the three dimensional cavity flow (z/D=0.5)

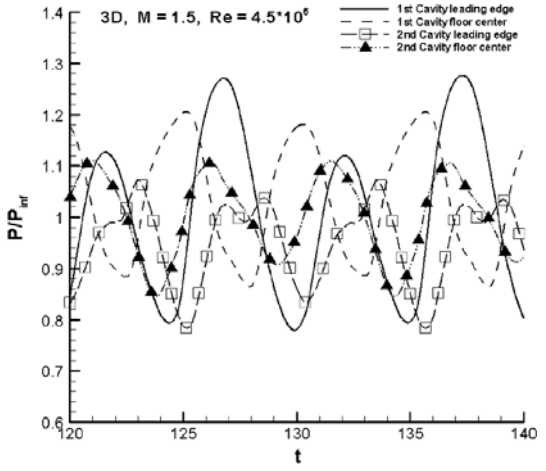

Fig. 6 Pressure histories at the three dimensional cavity flow (z/D=0.1)

centers of (x/D, y/D, z/D) = (1.5, 0.0, 0.5) and (4.5, 0.0, 0.5), respectively. As shown in Fig. 4, the amplitude of the pressure oscillation of the first cavity is about twice as high as that of the second cavity at the cavity leading edges. The pressure at the cavity floor center of the second cavity is slightly less than that at the center of the first cavity, but the amplitudes of the pressure oscillations are almost the same. Since the expansion wave at the leading edge of the first cavity oscillates, the amplitude at the location is much higher than those of other locations. However, the amplitude of other locations are almost the same. The periodic time (T_p) of pressure oscillation for the first cavity and second cavity is about 5.2. The turbulent shear layer formed at the leading edge of the first cavity passed the second cavity with only a slight pressure variation. Therefore, the pressure variation at the first cavity was directly observed at the second cavity. In general, although the amplitude of the pressure oscillation increases at the cavity entrance due to the oscillation of the expansion wave, the amplitudes and periods in the other regions become almost constant with only the flow-dependent phase shift. Figs. 5 and 6 show the fluctuating pressure histories at z/D=0.5 and 0.1 of the three dimensional flow which differs from two dimensional history, because of lateral inflow and outflow. The oscillation period is 10.4, which is twice that of two dimensional flow. The two kinds of pressure amplitudes appear alternately in one period. Although the amplitudes of pressure oscillation at the first and the second cavity are different, the oscillation periods are the same for both cases. Based on these results, the effect of pressure variation at the first cavity would directly appear at the second cavity for three dimensional flow as it did for two dimensional flow. Also, the pressure amplitude at the cavity floor center of z/D=0.5 is larger than that near the wall at z/D=0.1. The pressure amplitude of the two dimensional flow is about 30% larger than that of the three dimensional flow. Therefore, it can be inferred that there is less pressure variation in three dimensional flow because of the lateral inflow and outflow flux. The z-directional inflow and outflow can be confirmed with the streamlines in Fig. 11.

In the oscillation frequency analysis, FFT (Fast Fourier Transform) was used to analyze SPL (Sound Pressure Level), which is expressed in the following equation.

$$SPL = 20 \log_{10}\left[\frac{|p|}{p_{ref}}\right](dB) \qquad (2)$$

$$p_{ref} = 2 \times 10^{-5} (\mathrm{N/m^2})$$

Figures 7 and 8 for the frequency characteristics of the SPL show the dominant frequencies of the two dimensional and three dimensional flow,

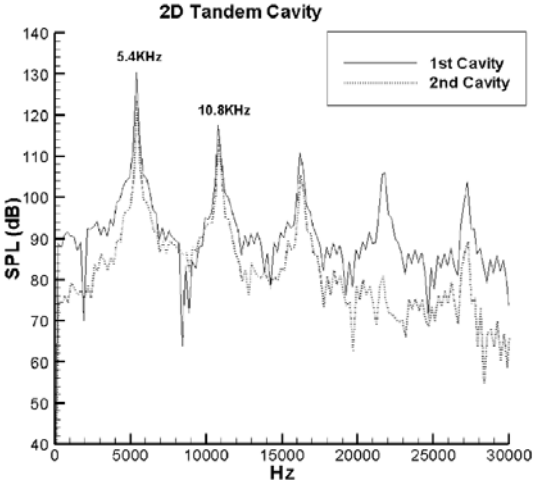

Fig. 7 SPL distribution for the two dimensional flow

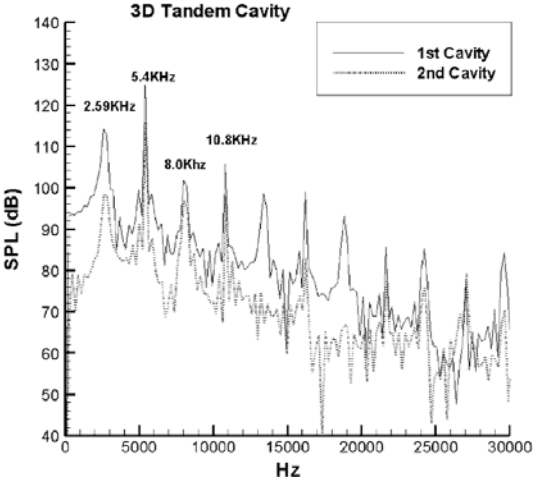

Fig. 8 SPL distribution for the three dimensional flow

respectively. The frequency characteristics of second cavity are the same as those of first cavity. These results show that the first cavity flows are transferred to the second cavities with only the phase shift. As shown in Fig. 8, the dominant frequency of three dimensional flow is 5.4 kHz, which is the same as that of two dimensional flow. However, there is another dominant frequency of 2.59 kHz due to the two kinds of pressure amplitudes, which appear alternately in three dimensional flow.

Table 1 shows the comparison of the frequency

Table 1 Comparison of dominant frequency (mode number $n=2$)

	Xin Zhang (1992, 1995)	Rossiter's Eq. (1964)	Two dimensional flow	Three dimensional flow
$L/D=3$	5.90 kHz	5.45 kHz	5.40 kHz	5.40 kHz

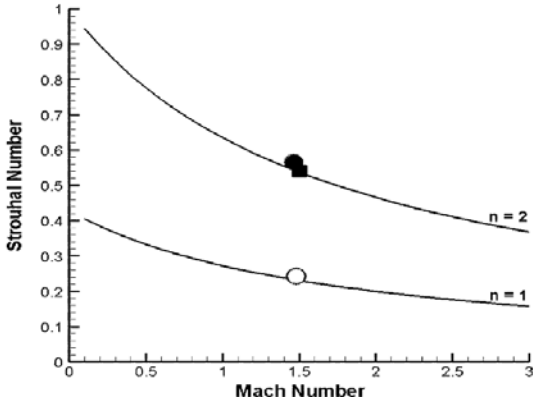

Fig. 9 Non-dimensional resonant frequencies as a function of Mach number, n=mode —: Rossiter's formula (1964), ■: $L/D=4$ (1971), ●: two dimensional result, ○: three dimensional result

characteristics of this study with the results of Rossiter's equation (1964) and Xin Zhang and Edwards (1995). The present results are very resonable.

Figure 9 shows the comparison of the non-dimensional Strouhal numbers (Rossiter, 1964) obtained by Eq. (3) with the experimental values of Heller (1971).

$$St=\frac{fL}{U}=\frac{n-\gamma}{1/k_v-M} \tag{3}$$

St is the non-dimensional Strouhal number. L is the cavity length (=45 mm), U is the real time freestream velocity (=432 m/s), n is the n^{th} oscillation mode, k_v(=0.57) is the constant representing the vortex convection speed as a fraction of the freestream flow speed at the cavity entrance, M is the freestream Mach number, and γ(=0.25) is a constant obtained from experiments (Chingwei and Philip, 2001). The Strouhal number of Heller (1971) is 0.6. The 2nd mode ($n=2$) Strouhal numbers calculated in this work for two dimen-

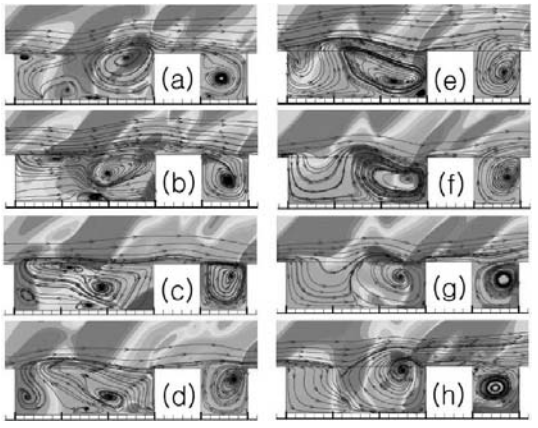

Fig. 10 Streamlines of the two dimensional flow (Total Time=5.2, Sampling Time=0.65, $M=1.5$, Re=4.5×10^5)

sional and three dimensional flows are 0.57, which are almost the same as Rossiter's formula (1964) and the experimental value of Heller (1971). In three dimensional flow, the 1st mode ($n=1$) Strouhal number is observed as 0.269, which is similar to the value of the 1st mode by Rossiter's formula (1964).

Figure 10 shows the streamlines of two dimensional flow for one cycle of non-dimensional time step of about 0.65.

(1) $t=0.0$(a): Large scale vortices developed at the trailing edge of the first cavity and at the second cavity. Small vortices are starting to develop at the leading edge of the first cavity.

(2) $t=0.65$(b): The vortices at the trailing edge of the first cavity flow into the second cavity. The vortices developed at the leading edge of the first cavity are gradually moving toward the trailing edge.

(3) $t=2.6$(d): The two large scale vortices at the leading and trailing edges of the first cavity combine.

(4) $t=3.9$(f): The vortices at the leading edge of the first cavity combine fully with those at the trailing edge, and the large scale vortices at the second cavity escape to the trailing edge.

As mentioned in Heller-Bliss (1975) as "the physical mechanism of flow-induced pressure fluctuations," the freestream shear layer changes

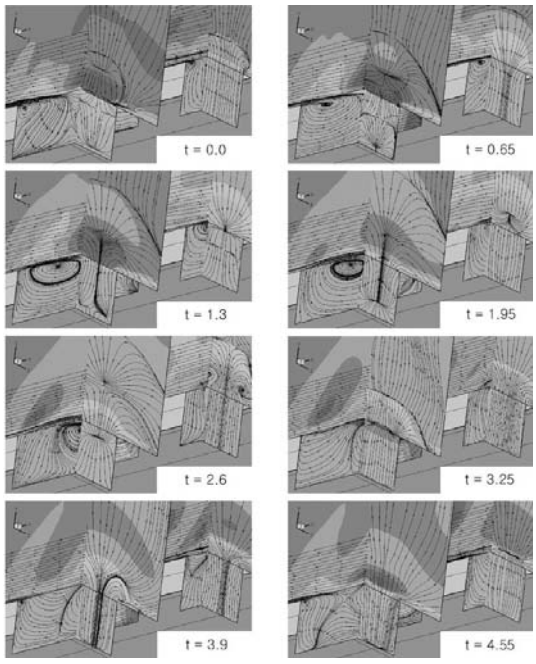

Fig. 11 Three dimensional streamlines (Total time=5.2, Sampling time=0.65, $x/D=1.5$, 4.5, $z/D=0.9$)

periodically and the flow moves periodically from the first cavity to the second cavity, according to the periodic repetition and movement of the large scale vortical structures.

Figure 11 shows the streamlines at the $x-y$ cross section of the inside of the three dimensional flow $z/D=0.9$ of for the first and the second cavity, and the streamlines at the $y-z$ cross section of $x/D=1.5$ and 4.5, respectively. The figures are useful to understand the three dimensional effect. In three dimensional flow as two dimensional flow, the freestream shear layer varies periodically with the periodic repetition and movement of the flow inside the cavities, so the flow from the first cavity repeatedly flows to the second cavity. Compared with two dimensional cavity flow, three dimensional cavity flows are less complex and has fewer vortices. The figures show that a downstream flow develops behind the vortices with a lateral inflow to the cavity when vortices are formed in the cavities. Also, when an upstream flow develops in front of the vortices, lateral flow from the cavity is expected to flow

out. The flow characteristics at the second cavity had the same periodicity as those of the first cavity. Lateral inflow occurred because of the downstream flow behind the vortices, and outflow occurred because of the upstream flow in front of the vortices. Small vortices formed and dissipated at the outside corners of the cavities because of the periodicity of the vortices inside the cavities. The figures show that formation and dissipation of vortices in the cavities and the oscillation period are the same for two dimensional and three dimensional flows. However, the flow pattern and pressure distribution of the two dimensional flow were much more complex and violent than those of the three dimensional flow.

In Fig. 12, the streamlines at the cavity floor show the reverse flow region and three dimensional separation flow. The figures show the saddle points and the limiting streamlines corresponding to the three dimensional separation.

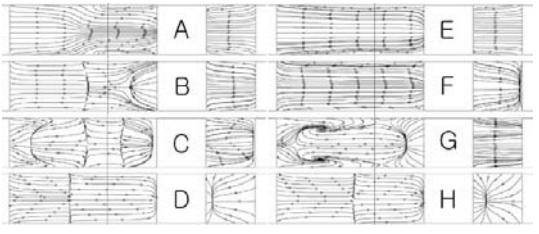

Fig. 12 Streamlines on the floor of cavities

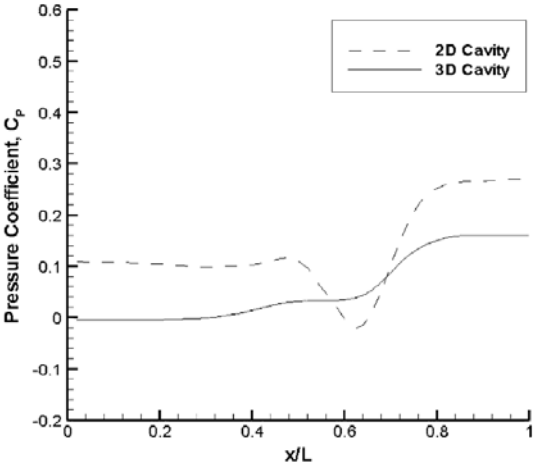

Fig. 13 Comparison of mean pressure coefficients on the fist cavities floor

Figure 13 shows the mean pressure distribution at the center lines of the 1st cavity floor for two dimensional and three dimensional flows. The pressure variation of the two dimensional flow was larger and more violent than that of the three dimensional flow. This phenomenon can be observed in the shear layer pattern in Fig. 14(a) and (b), which show the density contours of the two dimensional and three dimensional flows, respectively. The shear layer formed behind the second cavity of the two dimensional flow was thicker, and small vortices flow to downstream. On the other hand, the shear layer of the three dimensional flow was thinner than that of the two dimensional flow. This result represents the pattern of a general shear layer, which is similar to the results of Gharib and Roshko (1987). Gharib and Roshko (1987) confirmed that two dimensional flow changes from shear layer mode to wake mode as the L/D ratio increases and that shear layer mode is more dominant in three dimensional flow. In this calculation, the shear layer mode was observed in

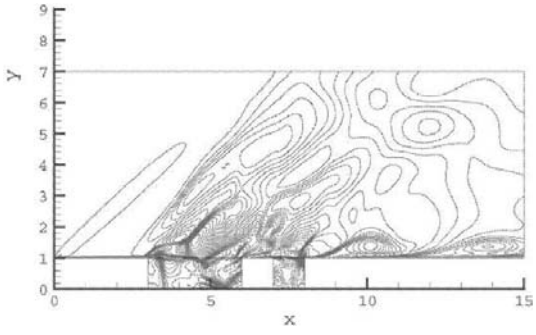

Fig. 14(a) Density contours of the two dimensional flow

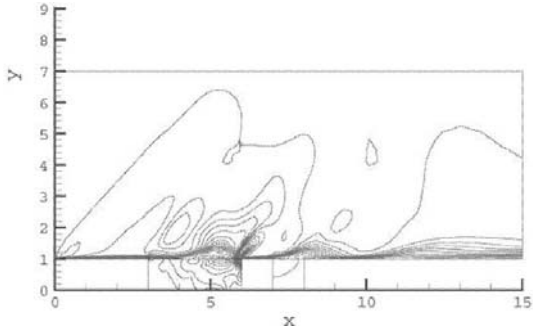

Fig. 14(b) Density contours of the three dimensional flow

both of two dimensional and three dimensional flow.

4. Conclusions

The characteristics of three dimensional cavity flows were simulated such as the generation and movement of vortices and the generation and dissipation of waves caused by the oscillation of the freestream shear layer around the tandem cavities by the unsteady Reynolds-Averaged Navier-Stokes (RANS) equation with $k-\omega$ turbulence model. Mach number of 1.5 and Reynolds number of 4.5×10^5 were used, the aspect ratios (L/D) of the first and second cavities were 3.0 and 1.0, respectively. The ratio of interval to depth (S/D) was 1.0, and the ratio of width to depth (W/D) for three dimensional flow was 1.0. The dominant oscillation frequency obtained by SPL frequency analysis coincided with the 2nd mode value of Rossiter's formula (1964) and experimental value of Xin Zhang and Edwards (1995), and the oscillation frequency corresponding to the 1st mode of Rossiter's formula was observed for three dimensional flow. The non-dimensional Shrouhal numbers were in agreement with the experimental values of Heller (1971) and the results of Rossiter's formula (1964). The oscillation characteristics of the two dimensional and three dimensional flows corresponded to shear layer mode. Although the shear layer at the leading edge diffused, it attached at the trailing edge, which caused the freestream flow did not mix violently with the cavity flow. Two dimensional flow was more violent than three dimensional flow because three dimensional flow can inflow and outflow laterally. The streamline distribution for the transverse cross section shows the lateral inflow and outflow mechanisms for one period. The second cavity is characterized by the oscillation characteristics of the first cavity with only the phase shift due to the flow transferring time.

The comparison of the pressure variations at several points in the cavity showed that the amplitude of the pressure variation at the leading edge of the first cavity was very large due to the expansion wave oscillation, and that the amplitudes of the other region was almost same with only the phase shift. The results of streamline on the cavity floor showed the flow phenomenon such as saddle points and limiting streamline, which indicate the reverse flow region and flow separation in three dimensional flow.

References

Abdol-Hamid, C. S., Lakshmanan, B. and Carlson, J. R., 1975, "Application of Navier-Stokes Code PAB3D With Turbulence Model to Attached and Separated Flows," *NASA Technical Paper 3480*.

Baysal, O. and Stallings, P. L., 1998, "Computational and Experimental Investigation of Cavity Flow Fields," *AIAA J.*, Vol. 26, No. 1.

Chingwei, M. S., Philip, J. M., 2001, "Comparison of Two- and Three-Dimensional Turbulent Cavity Flows," *AIAA 2001-0511*, A01-16385.

David, C. and Wilcox, 2000, "Turbulence Modeling for CFD," *DCW Industries*, pp. 121～122

Gharib, M. and Roshko, A., 1987, "The Effect of Flow Oscillations on Cavity Drag," *Journal of Fluid Mechanics*, Vol. 177, pp. 501～530.

Heller, H. H., Holmes, D. G. and Covert, E. E., 1971, "Flow-Induced Pressure Oscillations in Shallow Cavities," *Journal of Sound and Vibration*, Vol. 18, pp. 545～553.

Heller. H. H. and Bliss, D. B., 1975, "The physical mechanism of Flow-Induced Pressure Fluctuations in Cavities Concepts for Their Suppression," *AIAA-1975-491*.

Hoffmann, K. C. and Chiang, S. T., 1993, "Computational Fluid Dynamics for Engineers," *Engineering Education System USA*.

Hwang, S. W., 1994, "Navier-Stokes Simulation of Unsteady Supersonic Flow Over Double Cavity," *The Korean Society for Aeronautical and Space Sciences*, Vol. 22, No. 5.

Krishnamurty, K., 1995, "Acoustic Radiation From Two-Dimensional Rectangular Cutouts in Aerodynamic Surfaces," NACA, TN-3487.

Maull, D. J. and East, L. F., 1963, "Three-Dimensional Flow in Cavities," *Journal of Fluid Mechanics*, Vol. 16, pp. 620～632.

Pao, S. P. and Abdol-Hamid, K. S., 1996, "Nu-

merical Simulation of Jet Aerodynamics Using the Three- Dimensional Navier-Stokes Code PAB3D," *NASA Technical Paper 3596*.

Rossiter, J. E., 1964, "Wind-Tunnel Experiments on the Flow over Rectangular Cavities at Subsonic and Transonic Speeds," *Aeronautical Research Council Reports and Memoranda*, 3438.

SarKar, S., Erlebacher, G., Hussaini, M. Y. and Kreiss. H. O., 1991, "The Analysis and Modelling of Dilatational Terms in Compressible Turbulence," *J. Fluid Mech*., Vol. 227, pp. 473～493.

Woo, C. H. and Kim, J. S., 2005, "Two-And Three-Dimensional Supersonic Turbulent Flow Over a Single Cavity," *Korean Society of Computational Fluids Engineering*, Vol. 10, No. 4.

Xin Zhang and Edwards, J. A., 1992, "Experimental Investigation of Supersonic Flow over Two Cavities in Tandem," *AIAA J*., Vol. 30, No. 3.

Xin Zhang and Edwards, J. A., 1995, "Analysis of Unsteady Supersonic Cavity Flow employing an Adaptive Meshing Algorithm," *Computers and Fluids*, Vol. 25, No. 4.